Talanta 254 (2023) 124190

Contents lists available at ScienceDirect

Talanta

journal homepage: www.elsevier.com/locate/talanta

Electromechanical RT-LAMP device for portable SARS-CoV-2 detection

E. Alperay Tarim [a], Cemre Oksuz [a], Betul Karakuzu [a], Ozgur Appak [b], Ayca Arzu Sayiner [b], H. Cumhur Tekin [a,c,*]

[a] Department of Bioengineering, Izmir Institute of Technology, Izmir 35430, Turkey
[b] Department of Medical Microbiology, Dokuz Eylul University, Faculty of Medicine, Izmir 35330, Turkey
[c] METU MEMS Center, Ankara 06520, Turkey

ARTICLE INFO

Keywords:
SARS-CoV-2
Loop-mediated isothermal amplification (LAMP)
Point-of-care testing
Electromechanical systems
Colorimetric detection

ABSTRACT

Rapid point-of-care tests for infectious diseases are essential, especially in pandemic conditions. We have developed a point-of-care electromechanical device to detect SARS-CoV-2 viral RNA using the reverse-transcription loop-mediated isothermal amplification (RT-LAMP) principle. The developed device can detect SARS-CoV-2 viral RNA down to 10^3 copies/mL and from a low amount of sample volumes (2 μL) in less than an hour of standalone operation without the need for professional labor and equipment. Integrated Peltier elements in the device keep the sample at a constant temperature, and an integrated camera allows automated monitoring of LAMP reaction in a stirring sample by using colorimetric analysis of unfocused sample images in the hue/saturation/value color space. This palm-fitting, portable and low-cost device does not require a fully focused sample image for analysis, and the operation could be stopped automatically through image analysis when the positive test results are obtained. Hence, viral infections can be detected with the portable device produced without the need for long, expensive, and labor-intensive tests and equipment, which can make the viral tests disseminated at the point-of-care.

1. Introduction

RNA viruses are pathogenic organisms that cause important diseases in humans, and diagnostic tests are of great importance for the early diagnosis and treatment process of these viruses [1]. Immuno-based methods are performed based on capturing antibodies produced against the virus and are widely used but are not effective in the early detection of the virus [2]. With the spread of COVID-19, early detection methods have gained great importance in order to take timely preventive measures [3]. Although RT-qPCR has a high accuracy that is accepted as the gold standard method for COVID-19 detection, its usage is limited because it is a non-portable, laboratory-dependent, and high-cost test, and it also needs technical expertise for its operation [4]. On the other hand, LAMP tests are performed at a constant temperature, they eliminate the need for a thermal cycler and can offer a cost-effective analysis, unlike the RT-qPCR method [5]. The LAMP method, which has been widely used in studies for COVID-19 detection, has revealed sensitive and easy-to-use analysis [6]. Colorimetric detection can be used for LAMP tests, where the color change is appeared for a positive sample with an altered pH value due to the reaction [7]. For instance, the viral genome of SARS-CoV-2 could be detected in real-time by the RT-LAMP method [4]. With the use of this diagnostic method, by targeting ORF1ab and N regions of SARS-CoV-2 RNA performed on the heating block, 10^3 copies/mL limit of detection was reached using naked eye inspection in 25 min [8]. In another LAMP-based diagnostic system, an artificial SARS-CoV-2 genome was detected in real-time using microelectrodes [9]. In this portable platform supported by Arduino to control temperature and measure electrical potential, the presence of viral genome was studied in the 10-10^4 copies in a 50 μL sample by monitoring the pH change through the electrical potential that could increase the cost per test. RT-LAMP-based SARS-CoV-2 detection can also be performed using electrochemical sensors. For instance, disposable electrochemical test strips containing screen-printed electrodes were used for the detection of N and ORF1ab genes of the SARS-CoV-2 [10]. This sensor with a detection limit of 38×10^{-6} ng/μL was successfully tested in wastewater samples. Furthermore, a potentiometric device monitoring pH changes of the LAMP process was developed for point-of-care detection of SARS-CoV-2 [11]. The device could detect SARS-CoV-2 in 25 min with a limit of detection of 10^5 copies in 25 μL sample. Based on RT-LAMP, the Palm Germ-Radar (PaGeR) platform can

* Corresponding author. Department of Bioengineering, Izmir Institute of Technology, Izmir 35430, Turkey.
E-mail address: cumhurtekin@iyte.edu.tr (H.C. Tekin).

https://doi.org/10.1016/j.talanta.2022.124190
Received 12 September 2022; Received in revised form 6 December 2022; Accepted 8 December 2022
Available online 10 December 2022

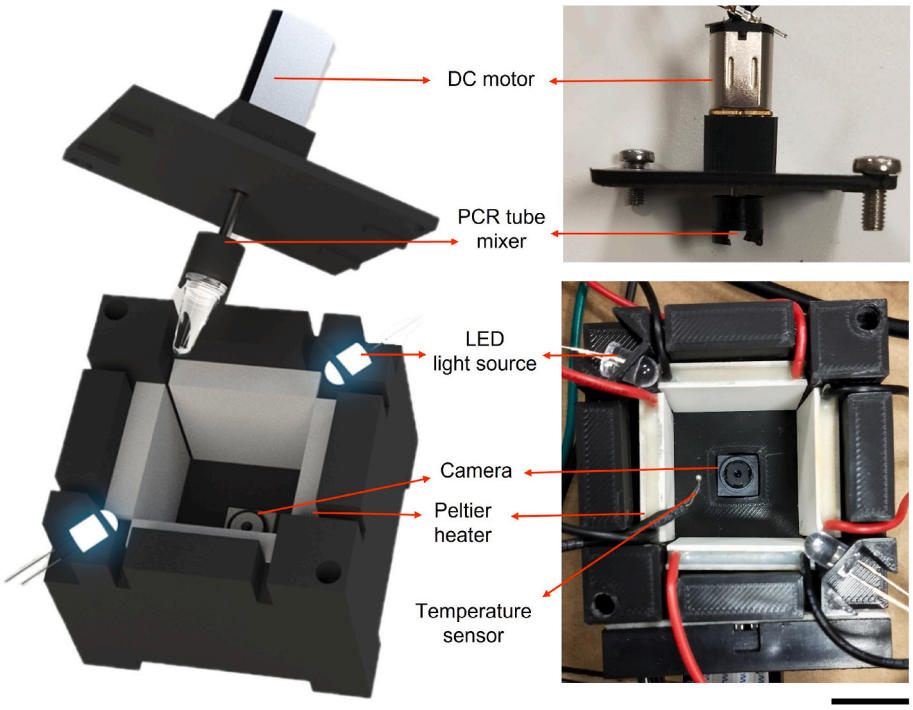

Fig. 1. Illustrations and photographs of automated LAMP analysis device for COVID-19 diagnosis. The device is composed of LEDs, Peltier heaters, a mixing apparatus, a DC motor, a temperature sensor, a camera, and a 3D-printed frame. The scale bar is 10 mm.

detect the COVID-19 viral genome down to 1-5 $\times 10^3$ copies/mL within 1 h with a naked-eye using three detection methods, which were colorimetric, fluorimetric, and lateral dipstick [12]. However, the platform could not enable real-time *in situ* quantitative monitoring. Furthermore, the handheld portable platform contains a single-use microfluidic cartridge integrated with ion-sensitive field-effect transistors (ISFET) to identify voltage changes due to pH variations in LAMP reaction [13]. Although the detection limit of 10 copies/reaction has been reached with 20 min of reaction, the high cost of cartridge due to ISFET could be a limiting issue. The detection limit is important for the diagnosis of COVID-19, since the viral load of the collected sample could be down to $\leq 10^3$ copies/mL in the early-stage of the infection [14]. This may result in tests that do not have a low detection limit giving false results in the first days of COVID-19. Although some methods were developed for COVID-19 detection, a complete solution for automated LAMP testing at the point-of-care is limited. Here, we present a new COVID-19 diagnostic device using the LAMP method with automatic image analysis to monitor color change in the sample for real-time detection of a low amount of viral RNA. This low-cost device offers portable, rapid, and automated viral RNA detection without the need for expensive instruments, and technical expertise.

2. Materials and methods

2.1. Template and primer design

The LAMP primers used in the device were designed for the N gene region of SARS-CoV-2 (GenBank Accession no: NC_045512, positions 28,285–28,529), where designed primers are highly conserved for different variants of SARS-CoV-2 (e.g., Delta B.1.617.2 (GenBank Accession no: OX000604.1), and Omicron BA.5.2 (GenBank Accession no: OP136952.1)) [15]. Forward outer primer (F3: TGGACCCCAAAATCAGCG), backward outer primer (B3: AGCCAATTTGGTCATCTGGA), forward inner primer (FIP: CGTTGTTTTGATCGCGCCCCATTACGTTTGGTGGACCCTC), backward inner primer (BIP: TACTGCGTCTTGGTTCACCGCATTGGAACGCCTTGTCCTC), forward loop primer (LF: TCCATTCTGGTTACTGCCAG), and backward loop primer (LB: GCAAGGAAGACCTTAAATTCCCTC) were initially designed using New England Biolabs (NEB) LAMP Primer Design Tool Version 1.0.1. All primers were synthesized (Triogen Biyoteknoloji, Turkey). As a positive control, a SARS-CoV-2 RNA positive sample of QCMD SARS-CoV-2 EQA, 2020 panel was used, while a sample carrying human cytomegalovirus DNA (CMV, QCMD Human Cytomegalovirus DNA EQA panel, 2019) and hepatitis C virus RNA (HCV, QCMD Hepatitis C Virus RNA EQA Programme, 2020) were chosen as negative controls. Nucleic acid extraction of both positive and negative controls was done by an EZ-1 virus mini kit (Qiagen, Germany). The specific amount of template RNA and negative controls carrying CMV DNA, and HCV RNA were obtained from QCMD standards sample code as SCV2_101S-04, CMVDNA19S-02, and HCVRNA20C1-01, respectively. SARS-CoV-2 RNA concentrations were adjusted by dilution of the known SCV2_101S-04 sample ($10^{4.29}$ copies/mL) in distilled water (dH_2O). The LAMP reaction mixture was prepared using 25 μL Warmstart Colorimetric LAMP 2X Master Mix (New England Biolabs, USA), 2.5 μL of primer mix containing 6 LAMP primers, 8 μL of dH_2O, and 2 μL of the sample. 2 μL of dH_2O was used instead of RNA sample as a blank group.

2.2. Fabrication of electromechanical device

The fabricated automated electromechanical device allows the amplification of the SARS-CoV-2 viral gene. The device's dimensions are kept small for portable operation (50 mm × 50 mm × 39.3 mm) (Fig. 1). SARS-CoV-2 viral gene detection is conducted on this device, which automatically analyses color change due to LAMP reaction at a constant temperature of 65 °C. As the LAMP reaction takes place, there is a color change from pink to yellow in the reaction solution. The temperature required for the LAMP reaction is supplied with four Peltier heaters (TEC1-04905, Thermonamic, China) surrounding the disposable PCR tube, where LAMP amplification takes place. It is hard to couple temperature sensors on the rotating PCR tube containing the sample. Here, a low-cost thermocouple temperature sensor (WRN-02B–NiCr–Ni Thermocouple, ISISO, Turkey) was used to monitor the temperature nearby

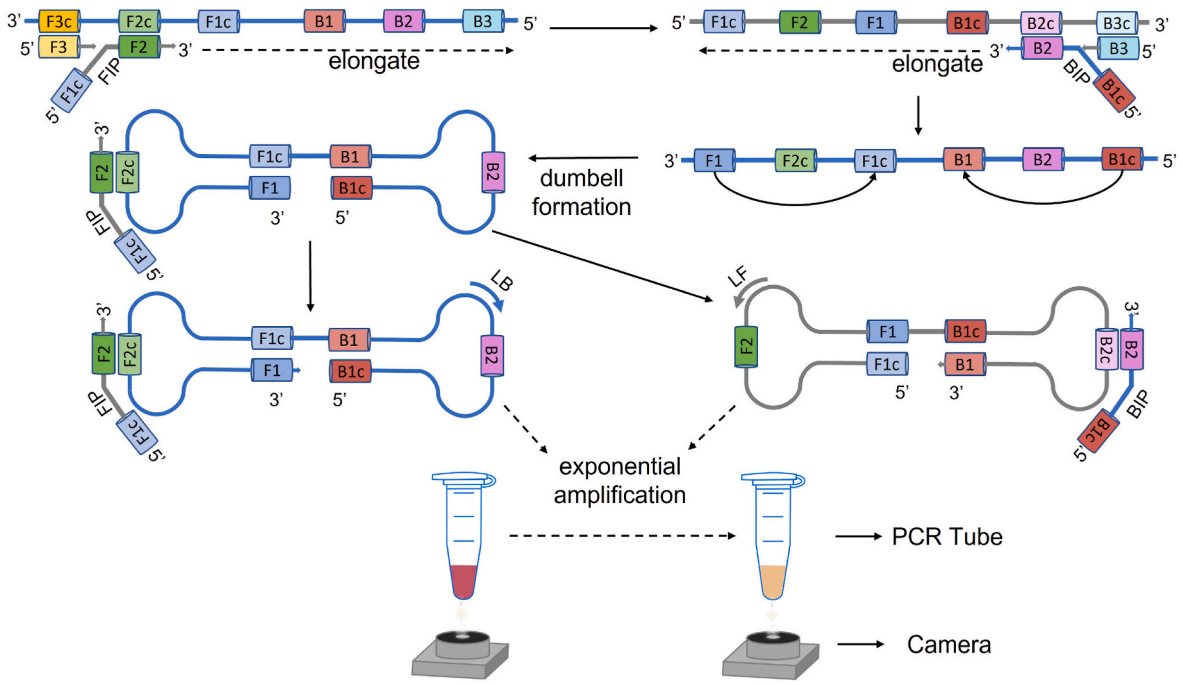

Fig. 2. The illustration of the RT-LAMP protocol conducted in the presented device. RT-LAMP protocol was realized in the PCR tube with F3/B3 (forward/backward outer primers), FIP/BIP (forward/backward inner primers), and LF/LB (forward/backward loop primers) for the exponential amplification. The color change in the PCR tube indicating the presence of SARS-CoV-2 RNA is monitored with a camera. (For interpretation of the references to color in this figure legend, the reader is referred to the Web version of this article.)

the rotating PCR tube during operation. Temperature is controlled with an Arduino microprocessor (Arduino Mega 2560 R3, Italy) using the temperature sensor and it is maintained at 65 ± 2 °C by powering on/off Peltier heaters automatically. The wiring schematic and control algorithm for temperature control were shown in Fig. S1 and Fig. S2, respectively. A DC motor (Micro Metal Gearmotor HPCB 3061, Pololu, USA), which is driven with 1.2 V, rotates the PCR tube at 300 rpm to mix the sample in order to accelerate LAMP amplification [16,17] and obtain a homogeneous color in the reaction tube [18]. The observations of LAMP amplification are done by taking the photos with the camera (Raspberry Pi Camera Module V2, Raspberry Pi, USA) from the bottom of the PCR tube. The camera is mounted 2.5 cm away from the bottom of the PCR tube, but it does not need to focus well on the tube which makes the device size minimum. Camera control and analysis of the obtained photos are made on a microcomputer (Raspberry Pi 3 B+, Raspberry Pi, USA). The lighting of the platform is maintained with two white LEDs (12383, Robotistan, Turkey), which are located at the opposite top corners of the platform and are operated with 5 V supplied from the microcomputer (Fig. S1). The technical drawing of the complete device is shown in Fig. S3.

2.3. Detection procedure

For the LAMP amplification, the device is first heated for 2 min to reach 65 °C and then the PCR tube containing the LAMP reaction mixture is mounted on the mixing apparatus found on the lid of the device (Video S1). After the lid is closed, sample mixing and LAMP reactions are initiated. LAMP uses forward outer primer (F3), backward outer primer (B3), forward inner primer (FIP), backward inner primer (BIP), backward loop primer (LB), and forward loop primer (LF) to recognize target RNA (Fig. 2). The amplification is initiated with the annealing of the inner primer to the target region which is then extended by RNA polymerase. The outer primer anneals to the original backbone to displace the product then reverse complementary sequences on the product anneals to each other and forms a self-hybridizing loop structure. This process goes with the displacement-annealing cycles to form a dumbbell structure. The dumbbell structure is a seed for the exponential LAMP amplification containing multiple initiations and annealing sites for primers. Thus, the amplification takes place in these multiple regions, and the products increase and form yellow color in the PCR tube for the detection [19]. The camera on the device starts to take photos of the PCR tube three times every 5 min for the entire amplification process without stopping the tube rotation.

Color analysis of the captured PCR tube photos is made in hue/saturation/value (HSV) color space by masking specific color intensity at a certain threshold [20,21]. As explained in Fig. S4 and Fig. S5, the captured images are first converted from the red-green-blue (RGB) color space matrix to the HSV color matrix with the color gamut conversion algorithm [22], and then they are processed to measure the yellow color intensity value indicating the presence of SARS-CoV-2. For this purpose, the HSV representation of the captured images are masked with the hue value (hue: >0.982 and < 0.257) for specifying the specific hue value of the yellow color, the brightness value (brightness: >1.0 and < 0.528) for masking unwanted dark and bright fields, and the saturation value (saturation: >1.0 and < 0.287) for determining the color change from pink to yellow due to the amplification. By doing so, positive samples can be identified with increased saturation value depending on the yellow color intensity. Each experiment was repeated 3 times and saturation values of experiments every 5 min were calculated as mean ± standard deviation (SD) by using the photo giving maximum saturation values from three consecutive photos of the PCR tube in each experiment.

3. Results and discussion

The device was tested at different rotational speeds to ensure optimum mixing for amplification without affecting HSV analysis on captured photos. 3 repeated photographs of yellow food dye in PCR tubes were captured with continuous rotation at 0, 100, 300, and 600 revolutions per minute (rpm). The observations show that rotational speeds up to 300 rpm did not affect the HSV analysis (Fig. 3). The HSV saturation value decreases due to the change in a blur of moving objects

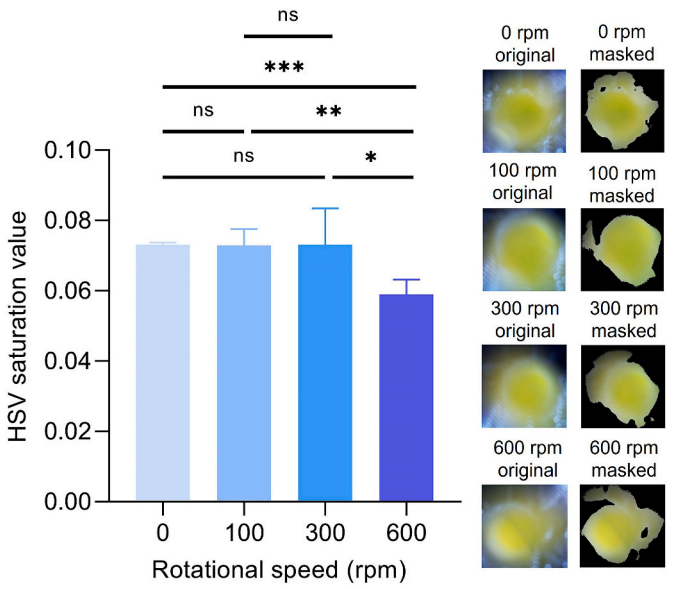

Fig. 3. HSV saturation values at different rotational speeds. HSV saturation values of the masked photographs taken at 0, 100, 300, and 600 rpm rotational speeds were measured. Data were calculated as the mean ± SD of 3 replicates of experiments. Statistical differences were obtained using a one-way ANOVA test at each rotational speed. The symbols (*), (**), and (***) represent $p < 0.05$, $p < 0.01$, and $p < 0.001$, respectively. ns means non-significant.

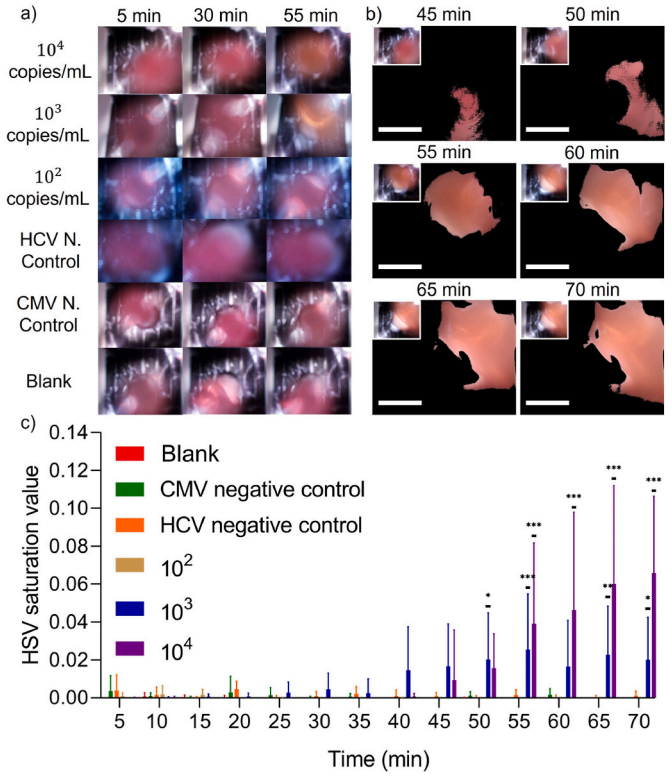

Fig. 4. Detection results obtained on the platform. (a) Unmasked raw photos of PCR tubes taken at 5th, 30th, and 55th min of the incubation time for different SARS-CoV-2 RNA concentrations (10^4 copies/mL, 10^3 copies/mL and 10^2 copies/mL), 2.5×10^6 copies/mL CMV sample (negative control), 1.98×10^3 copies/mL HCV sample (negative control), and blank group (0 copies/mL). (b) HSV masked images of the PCR tube having 10^4 copies/mL of SARS-CoV-2 RNA. The inset images show the unmasked raw photos. The scale bars are 2 mm. (c) Time-dependent graph of saturation values of HSV masked images. Data were shown as the mean ± SD of 3 replicates of experiments. Statistical differences were compared with the blank using a 2-way ANOVA test in each time set. The symbols (*), (**), and (***) represent $p < 0.05$, $p < 0.01$, and $p < 0.001$, respectively.

at 600 rpm rotational speed. Therefore, 300 rpm was chosen as the optimal mixing speed having a negligible effect on the HSV analysis that can allow real-time analysis without stopping the rotation. The reason for taking photos without stopping the mixing process is to model the real-time RNA detection process which could inform users immediately about the positive results without waiting for the whole pre-set duration of the LAMP process. The effect of the mixing procedure on the LAMP process was also examined. It was shown that the mixing process improved the difference between the detection signals of positive samples (Fig. S6).

Furthermore, camera to PCR tube distance was examined to show the effect of the camera focusing on HSV analyses. The HSV saturation value decreases as the PCR tube moves away from the camera in order to focus the photos. (Fig. S7). The camera to PCR tube distance should be set to 10 cm to get focused images that can enlarge the device size. Although a macro lens could be used to get focused photos at a shorter distance, this lens could increase the cost and the size of the device. On the other hand, the whole PCR tube is not visible at distances below 2.5 cm. Because of that camera to PCR tube distance is set to 2.5 cm in the device to get maximum HSV values.

The device was tested with different concentrations of SARS-CoV-2 RNA, negative controls carrying CMV DNA and HCV RNA, and the blank group without any nucleic acids. The color change started to be seen at 10^3 copies/mL (~15 fg/mL) and 10^4 copies/mL of SARS-CoV-2 RNA concentrations on PCR tube photos after 55 min (Fig. 4a). HSV masked images were also obtained from captured photos (Fig. 4b). The saturation values of HSV masked images were analyzed (Fig. 4c). A significant difference was observed for $\geq 10^3$ copies/mL of SARS-CoV-2 RNA after 50 min compared to blank and control groups. However, there was no significant difference at 10^2 copies/mL SARS-CoV-2 during 70 min of the whole amplification process. Due to used low sample volume of 2 μL, which is in the range of advised sample volume (2–10 μL) in the LAMP 2X Master Mix datasheet, the probability of RNA copies available inside the sample is low at this concentration level. This indicates that the detection limit of the platform is $\sim 10^3$ copies/mL. To decrease the detection limit further, the sample volume and also the LAMP reaction mixture could be increased but this would increase the cost per test.

Moreover, no statistical differences were obtained for the 2.5×10^6 copies/mL (~10 pg/mL) CMV sample and 1.98×10^3 copies/mL HCV sample (~10 fg/mL) used as negative controls with DNA and RNA viruses compared to the blank. Thus, used LAMP protocol allows high specificity for detecting SARS-CoV-2 RNA.

After 70 min of LAMP amplification for different samples, spectrometric measurements, which are also gold standards to analyze the color changes [23], were conducted. For this purpose, 12.5 μL of dH_2O was added to 37.5 μL of amplification solution to make up to 50 μL final solution to conduct absorbance measurements on a 96-well plate using a spectrophotometer (Multiscan Go, Thermo Fisher Scientific, USA). The spectrometric absorbance measurements between 300 and 800 nm wavelengths were shown in Fig. 5a. The amplifications gave peak values at around 432 and 560 nm wavelengths, since the wavelength of 432 nm, and 560 nm represent the intensity of the yellow and pinkish colors, respectively. The ratio of these two values (432 nm/560 nm) can measure how much color change occurs from pink to yellow in the amplification that can be used to quantify the RNA sample [24]. As shown in Fig. 5b, there were significant differences for $\geq 10^3$ copies/mL SARS-CoV-2 compared to control groups as in HSV analysis in the presented device. Moreover, 10^4 copies/mL of SARS-CoV-2 showed a higher detection signal, which was also observed in HSV analysis. Hence, instead of using an expensive spectrophotometer, a simple camera module combined with HSV analysis can be utilized for sensitive analysis of SARS-CoV-2 samples.

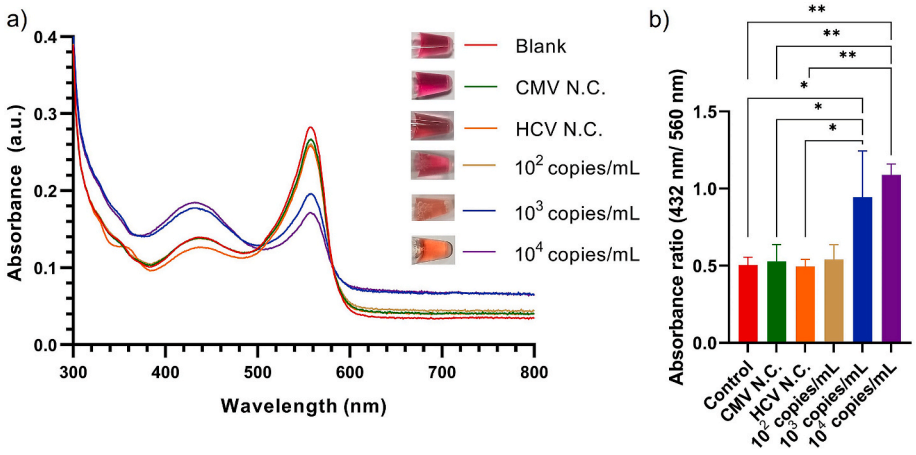

Fig. 5. Spectrometric measurements of LAMP mixture after amplification. (a) Absorbance graphs for different SARS-CoV-2 RNA concentrations (10^2-10^4 copies/mL), 2.5×10^6 copies/mL CMV sample (negative control), 1.98×10^3 copies/mL HCV sample (negative control), and blank group (0 copies/mL). The inset images show PCR tube photographs for different samples captured outside the device. Absorbance values are shown as the average of 3 replicates of experiments. (b) Absorbance ratio at the wavelengths of 432 nm and 560 nm. Data were shown as the mean ± SD of 3 replicates of experiments. Statistical differences were compared with the controls using one-way ANOVA by Holm-Sidak statistical hypothesis testing. The symbols (*) and (**) represent $p < 0.05$ and $p < 0.01$, respectively.

In addition, the device was tested with different SARS-CoV-2 concentrations to analyze the performance of the device for quantitative detection (Fig. 6). The analyses were conducted on images taken after 70 min of amplification. The limit of quantification (LOQ) signal was calculated as mean + 10 × SD of the mean of the HCV negative control group, which gives the highest detection signal among the control groups [25]. The HSV values for the concentration of $\geq 10^3$ copies/mL are bigger than LOQ, so these concentrations ($\geq 10^3$ copies/mL) could be sensed in the device. Although high standard deviation values were observed for different SARS-CoV-2 RNA concentrations, a linearity between the measured HSV saturation values and spiked RNA concentrations was seen (Fig. 6).

The comparison of the LAMP-based devices to detect SARS-CoV-2 was shown in Table S1. The presented device has solid features and qualifications for detecting SARS-CoV-2 RNA in terms of limit-of-detection, cost, and real-time monitoring. The limit-of-detection value of our device (10^3 copies/mL) is sufficient for diagnosis from swab samples at the early stage of infection [9]. The real-time detection feature of this device could terminate the protocol earlier depending on viral loads. Although electrochemical detection methods could improve the detection time further, these methods need special electrodes that should be disposed of after each test. On the other hand, colorimetric detection methods, which monitor only the color changes in the sample, could reduce the cost of tests by eliminating the need to dispose of high-cost detection sensors. Moreover, the integrated heater on the presented device could maintain the required temperature for LAMP process without external components. Automated readout could also be used to quantify SARS-CoV-2. These features ensure user-friendly and plug-and-play operation of the device.

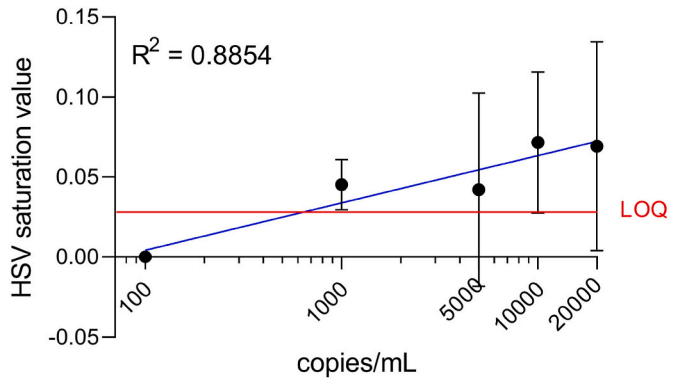

Fig. 6. The analyses in the device for different SARS-CoV-2 RNA concentrations at 70th minute of amplification. Data were shown as the mean ± SD of 3 replicates of experiments. The coefficient of determination (R^2) value calculated using semi-log regression analysis of the data was shown on the graph. R^2 was evaluated on the mean HSV saturation values of each concentration.

4. Conclusion

The proposed device was applied to detect SARS-CoV-2 RNA using LAMP protocols at a constant temperature with automatic and real-time colorimetric analysis. Real-time detection could reduce viral detection assay time of qualitative tests by terminating the LAMP amplification procedure when positive test results were observed. The device allows sensitive detection of viral RNA down to 10^3 copies/mL in ~55 min with low-cost components. In this way, it could permit early-stage COVID-19 detection with low detection limits. This affordable device costs less than $200 with low-cost components like Peltier heaters, DC motor, thermocouple temperature sensor, microcomputer, and camera and it requires only ~$2 per virus detection test. It can be 3D printed, assembled, and installed easily with accessible components even in remote rural regions. The device can detect viral RNA at point-of-care settings without the need for any professional equipment or personnel and is portable due to its small dimensions. Hence the device and the developed assay can provide rapid and point-of-care detection of COVID-19 and improve on-site monitoring of the infection. It provides a stable temperature for amplification and automated SARS-CoV-2 RNA detection with a mounted camera module at the bottom of the device using unfocused PCR tube photos. Although primers specific to the N gene of the SARS-COV-2 Wuhan-Hu-1 virus were used in the platform, primer sequences can be designed for other gene regions or different variants so that genomic changes can be tested, and other regions of the virus can be identified to obtain more precise results. The primers can also be designed for different viruses. Thus, this automated electromechanical device can be easily updated to detect viral RNA/DNA of interest, making it useable in future epidemics and pandemics.

Author contributions

E. Alperay Tarim: Conceptualization, Methodology, Software, Validation, Formal analysis, Investigation, Data curation, Writing – original draft, Visualization; **Cemre Oksuz:** Conceptualization, Methodology, Investigation, Writing – original draft; **Betul Karakuzu:** Conceptualization, Methodology, Investigation, Writing – original draft; **Ozgur Appak:** Methodology, Validation, Resources, Writing – review & editing; **Ayca Arzu Sayiner:** Methodology, Validation, Resources, Writing – review & editing; **H. Cumhur Tekin:** Conceptualization, Methodology, Resources, Formal analysis, Writing – original draft, Writing – review & editing, Supervision, Project administration, Funding acquisition.

Declaration of competing interest

The authors declare that they have no known competing financial interests or personal relationships that could have appeared to influence the work reported in this paper.

Data availability

Data will be made available on request.

Acknowledgements

H.C.T. would like to thank the Outstanding Young Scientists Award funding (TUBA GEBIP 2020) from the Turkish Academy of Science, Young Scientist Awards (BAGEP 2022) from Science Academy (Bilim Akademisi) and the scientific research project (2020IYTE0042) funded by Izmir Institute of Technology (IZTECH). B.K. and E.A.T. acknowledge the support of The Scientific and Technological Research Council of Turkey for the 2211-A BIDEB doctoral scholarship and the support of the Turkish Council of Higher Education for the 100/2000 CoHE doctoral scholarship. The authors would like to thank Engin Ozcivici, Ph.D. and Humeyra Taskent Sezgin, Ph.D. from the Department of Bioengineering, IZTECH, and Meltem Elitas, Ph.D. from the Department of Mechatronics Engineering, Sabanci University for helpful discussions.

Appendix A. Supplementary data

Supplementary data to this article can be found online at https://doi.org/10.1016/j.talanta.2022.124190.

References

[1] A. Cassedy, A. Parle-McDermott, R. O'Kennedy, Virus detection: a review of the current and emerging molecular and immunological methods, Front. Mol. Biosci. 8 (2021), 637559.
[2] B.D. Kevadiya, J. Machhi, J. Herskovitz, M.D. Oleynikov, W.R. Blomberg, N. Bajwa, D. Soni, S. Das, M. Hasan, M. Patel, Diagnostics for SARS-CoV-2 infections, Nat. Mater. 20 (2021) 593–605.
[3] E.A. Tarim, B. Karakuzu, C. Oksuz, O. Sarigil, M. Kizilkaya, M.K.A.A. Al-Ruweidi, H.C. Yalcin, E. Ozcivici, H.C. Tekin, Microfluidic-based virus detection methods for respiratory diseases, Emergent Mater 4 (2021) 143–168.
[4] J. García-Bernalt Diego, P. Fernández-Soto, M. Domínguez-Gil, M. Belhassen-García, J.L.M. Bellido, A. Muro, A simple, affordable, rapid, stabilized, colorimetric, versatile RT-LAMP assay to detect SARS-CoV-2, Diagnostics 11 (2021) 438.
[5] L. Mautner, C.-K. Baillie, H.M. Herold, W. Volkwein, P. Guertler, U. Eberle, N. Ackermann, A. Sing, M. Pavlovic, O. Goerlich, Rapid point-of-care detection of SARS-CoV-2 using reverse transcription loop-mediated isothermal amplification (RT-LAMP), Virol. J. 17 (2020) 1–14.
[6] J.J. Schellenberg, M. Ormond, Y. Keynan, Extraction-free RT-LAMP to detect SARS-CoV-2 is less sensitive but highly specific compared to standard RT-PCR in 101 samples, J. Clin. Virol. 136 (2021), 104764.
[7] M.N. Aoki, B. de Oliveira Coelho, L.G.B. Góes, P. Minoprio, E.L. Durigon, L. G. Morello, F.K. Marchini, I.N. Riediger, M. do Carmo Debur, H.I. Nakaya, Colorimetric RT-LAMP SARS-CoV-2 diagnostic sensitivity relies on color interpretation and viral load, Sci. Rep. 11 (2021) 1–10.
[8] E. Li, A. Larson, A. Kothari, M. Prakash, Handyfuge-LAMP: Low-Cost and Electricity-free Centrifugation for Isothermal SARS-CoV-2 Detection in Saliva, MedRxiv, 2020.
[9] M.M. Alvarez, S. Bravo-González, E. González-González, G. Trujillo-de Santiago, Portable and label-free quantitative loop-mediated isothermal amplification (LF-qLamp) for reliable COVID-19 diagnostics in three minutes of reaction time: arduino-based detection system assisted by a pH microelectrode, Biosensors 11 (2021) 386.
[10] R.G. Ramírez-Chavarría, E. Castillo-Villanueva, B.E. Alvarez-Serna, J. Carrillo-Reyes, R.M. Ramírez-Zamora, G. Buitrón, L. Alvarez-Icaza, Loop-mediated isothermal amplification-based electrochemical sensor for detecting SARS-CoV-2 in wastewater samples, J. Environ. Chem. Eng. 10 (2022), 107488.
[11] Q. Li, Y. Li, Q. Gao, C. Jiang, Q. Tian, C. Ma, C. Shi, Real-time monitoring of isothermal nucleic acid amplification on a smartphone by using a portable electrochemical device for home-testing of SARS-CoV-2, Anal. Chim. Acta 1229 (2022), 340343.
[12] A. Ge, F. Liu, X. Teng, C. Cui, F. Wu, W. Liu, Y. Liu, X. Chen, J. Xu, B. Ma, A Palm Germ-Radar (PaGeR) for rapid and simple COVID-19 detection by reverse transcription loop-mediated isothermal amplification (RT-LAMP), Biosens. Bioelectron. 200 (2022), 113925.
[13] J. Rodriguez-Manzano, K. Malpartida-Cardenas, N. Moser, I. Pennisi, M. Cavuto, L. Miglietta, A. Moniri, R. Penn, G. Satta, P. Randell, Handheld point-of-care system for rapid detection of SARS-CoV-2 extracted RNA in under 20 min, ACS Cent. Sci. 7 (2021) 307–317.
[14] F. Carrouel, M. Valette, E. Gadea, A. Esparcieux, G. Illes, M.E. Langlois, H. Perrier, C. Dussart, P. Tramini, M. Ribaud, Use of an antiviral mouthwash as a barrier measure in the SARS-CoV-2 transmission in adults with asymptomatic to mild COVID-19: a multicentre, randomized, double-blind controlled trial, Clin. Microbiol. Infect. 27 (2021) 1494–1501.
[15] P. Laine, H. Nihtilä, E. Mustanoja, A. Lyyski, A. Ylinen, J. Hurme, L. Paulin, S. Jokiranta, P. Auvinen, T. Meri, SARS-CoV-2 variant with mutations in N gene affecting detection by widely used PCR primers, J. Med. Virol. 94 (2022) 1227–1231.
[16] L. Lillis, J. Siverson, A. Lee, J. Cantera, M. Parker, O. Piepenburg, D.A. Lehman, D. S. Boyle, Factors influencing Recombinase polymerase amplification (RPA) assay outcomes at point of care, Mol. Cell. Probes 30 (2016) 74–78.
[17] G. Zheng, Q. Gao, Y. Jiang, L. Lu, J. Li, X. Zhang, H. Zhao, P. Fan, Y. Cui, F. Gu, Instrumentation-compact digital microfluidic reaction interface-extended loop-mediated isothermal amplification for sample-to-answer testing of Vibrio parahaemolyticus, Anal. Chem. 93 (2021) 9728–9736.
[18] B. Karakuzu, E.A. Tarim, C. Oksuz, H.C. Tekin, An electromechanical lab-on-a-chip platform for colorimetric detection of serum creatinine, ACS Omega 7 (2022) 25837–25843.
[19] M. Daskou, T.G. Dimitriou, D.S. Alexopoulou, D. Tsakogiannis, G.D. Amoutzias, D. Mossialos, Z. Kyriakopoulou, P. Markoulatos, WarmStart colorimetric RT-LAMP for the rapid, sensitive and specific detection of Enteroviruses A–D targeting the 5′ UTR region, J. Appl. Microbiol. 130 (2021) 292–301.
[20] L.-S. Yu, S.-Y. Chou, H.-Y. Wu, Y.-C. Chen, Y.-H. Chen, Rapid and semi-quantitative colorimetric loop-mediated isothermal amplification detection of ASFV via HSV color model transformation, J. Microbiol. Immunol. Infect. 54 (2021) 963–970.
[21] B. Karakuzu, E.A. Tarim, C. Oksuz, H.C. Tekin, An electromechanical lab-on-a-chip platform for colorimetric detection of serum creatinine, ACS Omega 7 (2022) 25837–25843.
[22] A.R. Smith, Color gamut transform pairs, ACM Siggraph Computer Graphics 12 (1978) 12–19.
[23] M.A. Lalli, J.S. Langmade, X. Chen, C.C. Fronick, C.S. Sawyer, L.C. Burcea, M. N. Wilkinson, R.S. Fulton, M. Heinz, W.J. Buchser, Rapid and extraction-free detection of SARS-CoV-2 from saliva by colorimetric reverse-transcription loop-mediated isothermal amplification, Clin. Chem. 67 (2021) 415–424.
[24] Y. Zhang, G. Ren, J. Buss, A.J. Barry, G.C. Patton, N.A. Tanner, Enhancing colorimetric loop-mediated isothermal amplification speed and sensitivity with guanidine chloride, Biotechniques 69 (2020) 178–185.
[25] B. Karakuzu, Y. Gulmez, H.C. Tekin, Absorbance-based detection of arsenic in a microfluidic system with push-and-pull pumping, Microelectron. Eng. 247 (2021), 111583.